Progress In Electromagnetics Research M, Vol. 50, 169–181, 2016

Multi-Beam Ring Antenna Arrays Synthesis by the Application of Adaptive Particle Swarm Optimization

Hichem Chaker[1, *], Mehadji Abri[2], and Hadjira Abri Badaoui[3]

Abstract—This paper describes the original results obtained in the field of multi-beam annular ring antenna array pattern synthesis for the modes TM_{11} and TM_{12}, by applying an iterative algorithm for phased arrays, which is able to produce low side-lobe levels patterns with multiple prescribed main lobes. The ring antenna analysis builds on the modified cavity model; this letter permits to take account of the fringing field effects by virtue of the dynamic permittivity. The proposed method is based on the adaptive particle swarm optimization algorithm. This solution is characterized by its simple implementation and a reduced computational time to achieve the desired radiation patterns. These advantages make the presented algorithm suitable for a wide range of communication systems. The original results obtained in the field of antenna array pattern synthesis are presented to illustrate the performance of the proposed method.

1. INTRODUCTION

Recently, antenna arrays have become a fundamental element in modern communication systems due to the thorough technological advances in this domain and the fast growing demand [1–4]. The ring printed antennas are well known for their multiband abilities and advantageous characteristics. They are used in communication systems, and several structures have been recently proposed in the literature [5]. Much attention has been given to the annular ring when it is used in its fundamental TM_{11} mode [6]. This printed antenna is smaller than its rectangular or circular counterparts. The annular ring may be a broadband antenna when operated near the TM_{12} resonance [7]. It has been established that the structure is a good resonator (with very little radiation) for TM_{1m} modes (m odd), and a good radiator for TM_{1m} modes (m even) [8]. As reported in the literature, the new meta-heuristic methods have found application in a great number of communication systems; they have increased the involvement of the research community in the synthesis of micro-strip antenna arrays. The literature counts a number of synthesis methods, such as Modified Spider Monkey Optimization [9], Artificial Neural Network Algorithm [10], Grey Wolf Optimization [11], to name but a few. The algorithms employed ought to produce radiation models with multiple main lobes to the selected directions and for certain practical applications, they should be able to carry out the synthesis by acting on the two parameters, i.e., the amplitudes and phases of excitations for both modes TM_{11} and TM_{12}. A great number of amplitude-phase techniques exist. The solutions that can give patterns with multiple main lobes are usually formulated for arrays having a square radiator [12, 13].

An efficient method for the pattern synthesis of linear and planar multibeam annular ring antenna arrays is presented in this paper. A multibeam pattern is realized by determining the excitation magnitude and phase of each array element, for the two modes TM_{11} and TM_{12}. The method suggested in the present work is based on the adaptive particle swarm optimization, and the linear and planar

Received 22 June 2016, Accepted 19 September 2016, Scheduled 5 October 2016

* Corresponding author: Hichem Chaker (mh_chaker2005@yahoo.fr).

[1] Electrical Engineering Faculty, University Djillali Liabes of Sidi Bel Abbès, Algeria. [2] LTT Laboratory, Department of Telecom, Tlemcen's University, Algeria. [3] STIC Laboratory, Telecom Department, University of Tlemcen, Algeria.

antenna array synthesis was modeled as a mono-objective optimization problem. The advantage of the adaptive particle swarm optimization algorithm over other existing algorithms lies in the pseudo code of APSO which generates new fresh particles after a number of iteration cycles to increase diversity of solutions. This helps prevent revisiting the same solutions for several times; it also provides better searching ability. In contrast to recent evolutionary algorithms, the particle swarm optimization is a simple method that comprises a combination of local and global search features. It therefore furnishes fast convergence [3, 14–17]. As such, this paper presents the application of an improved version of the particle swarm optimization algorithm, labeled *the adaptive particle swarm optimizer* with the aim of synthesizing linear and planar multi beams annular ring antenna array patterns for the TM_{11} and TM_{12} modes. To check the validity of the technique, a number of illustrative examples are simulated, and multi-beam patterns are demonstrated.

In terms of organization, the paper is structured in four sections. Section 2 presents the theoretical formulation and the basic equations to model the antennas array. Overviews of the adaptive particle swarm optimization algorithm are described in Section 3. Section 4 is a space where the results of the synthesis process are portrayed. Section 5 yields conclusions of the case study.

2. THEORETICAL CONSIDERATIONS

The present paper goes around the application of an annular-ring microstrip antenna to TM_{11} and TM_{12} modes at the resonance frequencies 0.6 GHz and 2.6 GHz, respectively. Figure 1, sketched below, shows the employed annular ring in the reference plane xyz. The antenna is energized via a coaxial probe at a distance ρ_0.

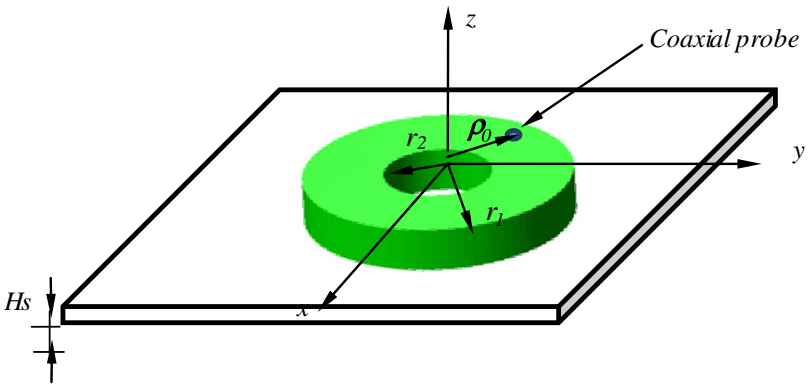

Figure 1. Geometry of an annular ring microstrip antenna.

An array antenna can be defined as a collection of individual elements in which the location and feeding are properly selected such that to enforce a desired far field pattern. Usually, array antennas are used when it is important to have a directive beam [18]. The far field annular ring antenna in the plane is expressed by the Equations (1) and (2) [19–21].

$$E_\theta = -j^n \frac{E_0 e^{-jK_0 H_S}}{2r} \left\{ \begin{array}{l} r_{2eq} A_n(K_0 r_{2eq} \sin\theta) F_{nm}(r_{2eq}) \\ -r_{1eq} A_n(K_0 r_{1eq} \sin\theta) F_{nm}(r_{1eq}) \end{array} \right\} \cos(n\varphi) \quad (1)$$

$$E_\varphi = -j^n \frac{E_0 e^{-jK_0 H_S}}{2r} \left\{ \begin{array}{l} r_{2eq} B_n(K_0 r_{2eq} \sin\theta) F_{nm}(r_{2eq}) \\ -r_{1eq} B_n(K_0 r_{1eq} \sin\theta) F_{nm}(r_{1eq}) \end{array} \right\} \sin(n\varphi)\cos(\theta) \quad (2)$$

$$A_n(\rho) = J_{n-1}(\rho) - J_{n+1}(\rho) \quad (3)$$

$$B_n(\rho) = J_{n-1}(\rho) + J_{n+1}(\rho) \quad (4)$$

$$F_{nm}(\rho) = J_n(K_{nm}\rho) Y_n'(K_{nm} r_1) - J_n'(K_{nm} r_1) Y_n(K_{nm}\rho) \quad (5)$$

K_0 is the wave number, and K_{nm} corresponds to the roots of the characteristic equation defined in (6). J_n and Y_n refer to the Bessel and Newman functions of the first kind and n order, respectively.

Their respective first derivatives K_{nm} is the resonant wave numbers. The boundary conditions for $\rho = r_2$. The dispersion equation for the resonance modes is written as follows:

$$J'_n(K_{nm}r_2)\,Y'_n(K_{nm}r_1) - J'_n(K_{nm}r_1)\,Y'_n(K_{nm}r_2) = 0 \tag{6}$$

To take account of the fringing fields along the ring edges, it is necessary to replace the ring internal and external rays by their equivalent values r_{1eq} and r_{2eq}.

$$r_{1eq} = \frac{r_1 + r_2 - w_{eff}(f)}{2} \tag{7}$$

$$r_{2eq} = \frac{r_1 + r_2 + w_{eff}(f)}{2} \tag{8}$$

$$w_{eff}(f) = (r_2 - r_1) + \frac{w_{eff}(0) - (r_2 - r_1)}{1 + \left(\frac{f}{f_p}\right)^2} \tag{9}$$

$$f_p = \frac{c_0}{w_{eff}(0)\sqrt{\varepsilon_{eff}}} \tag{10}$$

c_0 is the light speed in the vacuum, as shown below:

$$w_{eff}(0) = C_0 H_S \eta_0 c_0 \tag{11}$$

C_0 is identified with C for $\varepsilon_r = 1$. The effective permittivity is defined as: $\varepsilon_{eff} = \frac{C}{C_0}$.

C refers to the dynamic capacity resulting from the effect edges. It is determined by the dyadic green function as shown below:

$$\frac{1}{C} = \frac{1}{\pi\varepsilon_0}\int_0^\infty \left|\frac{\tilde{f}(\beta)}{Q}\right|^2 \tilde{G}(\beta)\frac{d(\beta H_S)}{\beta H_S} \tag{12}$$

$$\tilde{G}(\beta) = \frac{1}{\beta(1 + \varepsilon_r \coth(\beta H_s))}. \tag{13}$$

$$\frac{\tilde{f}(\beta)}{Q} = \frac{8}{5}\frac{\sin\left(\beta\frac{L}{2}\right)}{\beta\frac{L}{2}} + \frac{12}{5}\left(\beta\frac{L}{2}\right)^{-2}\left\{\cos\left(\beta\frac{L}{2}\right) - \frac{\sin\left(\beta\frac{L}{2}\right)}{\beta\frac{L}{2}} + \frac{\sin^2\left(\beta\frac{L}{2}\right)}{\left(\beta\frac{L}{4}\right)^4}\right\} \tag{14}$$

$L = r_2 - r_1$ and $\beta = \frac{2\pi}{\lambda_0}\sqrt{\varepsilon_r}$.

The far field radiated in free space from a linear array (1-D), composed of N identical sources of the directivity diagram $\vec{f}(\theta, \varphi)$, each one localized at position x_i can be written as:

$$F_{1D}(\theta) = \sum_{n=1}^{N} f(\theta) a_n \cos[K_0 x_n \cos(\theta) + \emptyset_n] \tag{15}$$

θ is the angular direction. a_n and $\emptyset_n$ represent the excitation amplitude and phase of each element complex weight, which has to be determined in case complex synthesis is considered. It should be mentioned that the mutual coupling effect between the elements was neglected in this paper. Also, the distance between adjacent elements was fixed $\Delta x = \Delta y = 0.5\lambda$. Figure 2 depicts the geometry of the linear annular ring antennas array.

For the planar array case, the directivity pattern $F(\theta, \varphi)$ is a function of the two direction angles θ and φ. If φ is fixed, the pattern $F(\theta, \varphi)$ could be conformed in the E plane or H plane. We are interested in the synthesis of linear arrays in the plane $\varphi = 0°$. An antenna array, which consists of M rows and N columns of elements, arranged along a rectangular grid in the xoy plane, is shown in Figure 3. The array has an element spacing of Δx in the x-direction and Δy in the y-direction. The far field can be expressed as follows:

$$F(\theta, \varphi) = f(\theta, \varphi)\sum_{m=1}^{Nx}\sum_{n=1}^{Ny} W_{mn} e^{jK_0 \sin\theta(X_m \cos\varphi + Y_n \sin\varphi)} \tag{16}$$

$$W_{mn} = W_m \times W_n \tag{17}$$

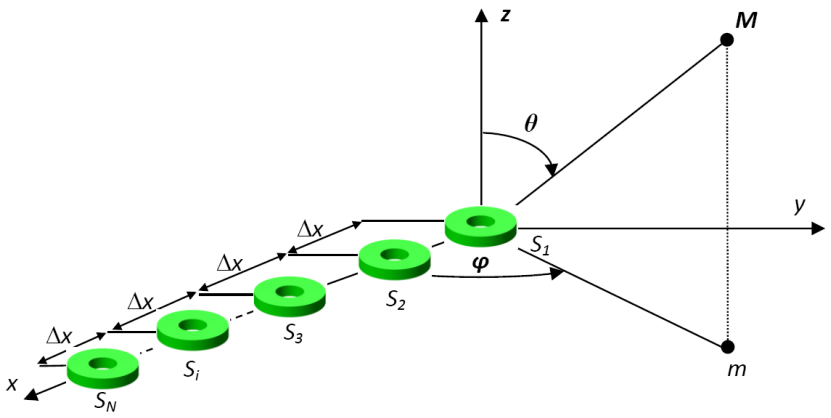

Figure 2. Linear ring antennas array.

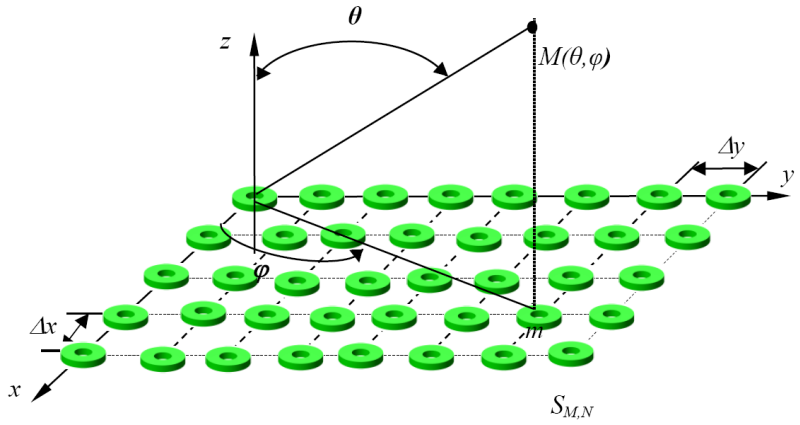

Figure 3. Element layout of uniform planar array.

where W_{mn} is the 2-D weight distribution of the array.

The elements amplitudes a_m and phases $\emptyset_m$ are related by the complex excitation weight $w_m = a_m e^{-j\emptyset_m}$ according to *Ox direction* and the elements amplitudes a_n and phases $\emptyset_n$ are related by the complex excitation weight $w_n = a_n e^{-j\emptyset_n}$ according to *Oy direction.*

The array factor in dB is given by:

$$P(\theta, \varphi) = 20\text{Log}(F(\theta, \varphi)_{normalized}) \tag{18}$$

The mathematical statement of the optimization process is:

$$\text{Find} \quad \max f(v) \rightarrow v_{opt} \tag{19}$$

where $f(v)$ is the objective function of parameter variables v, and v_{opt} is the optimal vector of solutions $(a_1, a_2, \ldots, a_N)$ in the case of the amplitude synthesis; it is equal to $(a_1, a_2, \ldots, a_N, \emptyset_1, \emptyset_2, \ldots, \emptyset_N)$ in the case of amplitude phase synthesis.

The optimization process can be modeled by minimizing the difference between the desired and calculated patterns. Mathematically, the optimization problem can be written as:

$$f = \text{Max} - \int_0^{\pi}\int\int |F_d(\theta, \varphi) - F(\theta, \varphi)| d\theta d\varphi \tag{20}$$

$F_d(\theta, \varphi)$ represents the desired pattern, and $F(\theta, \varphi)$ refers to the calculated pattern.

3. ADAPTIVE PARTICLE SWARM ALGORITHM

Modern heuristic algorithms are considered as practical tools for nonlinear optimization problems, which do not require the objective function to be differentiable or continuous.

A modified version of the standard PSO was employed for the optimal design of linear and planar arrays. The blessing of the adaptive particle swarm optimization (hereafter APSO) algorithm over other algorithms is a question of the pseudo code of APSO which generates fresh particles after a number of iteration cycles. This is of paramount importance as it avoids revisiting the same solution, and it offers a better probing ability. The particle swarm optimization algorithm, as discussed by Xiao [22], is an evolutionary computation technique, which is inspired by social behavior of swarms. PSO is similar to the other evolutionary algorithms, i.e., the system is initialized with a population of random solutions. Each solution or particle flies in a D-dimensional space with a dynamically adjusted speed. It is important to take into account the best position of the particle and the best positions of the particles of the neighborhood. The location of the ith particle is represented as $X_i = (x_{i1}, \ldots, x_{id}, \ldots, x_{iD})$. The best previous position (which gives the best fitness value) of the ith particle is recorded and represented as $P_i = (p_{i1}, \ldots, p_{id}, \ldots, p_{iD})$, which is also called *pbest*. The index of the best *pbest* among all the particles is represented by the symbol g. The location P_g is also called *gbest*. The velocity of the ith particle is represented as $V_i = (v_{i1}, \ldots, v_{id}, \ldots, v_{iD})$. The particle swarm optimization consists of, at each time step, changing the velocity and location of each particle toward its *pbest* and *gbest* locations according to Equations (21) and (22), respectively:

$$V_{id} = w \times V_{id} + C_1 \times rand() \times (p_{id} - x_{id}) + C_2 \times rand() \times (p_{gd} - x_{id}) \tag{21}$$

$$x_{id} = x_{id} + V_i \tag{22}$$

w is the inertia weight, C_1 and C_2 the acceleration constants, as discussed by Eberhart and Shi [23], and *rand ()* is a uniform random function in the range [0, 1]. In Equation (21), the first addend represents the inertia of the previous velocity; the second addend is the cognition addend, which represents the private thinking by itself, and the third addend is the social addend, which represents the cooperation among the particles, as discussed by Kennedy [24, 25]. V_i is clamped to a maximum velocity $V_{\max} = (v_{\max,1}, \ldots, v_{\max,d}, \ldots v_{\max,D})$. $V_{\max}$ determines the resolution with which regions between the present and the target position are searched, as discussed by Eberhart and Shi [23] Instead of specifying a starting point for the algorithm, we defined the limits of the input variables that the optimizer is allowed to search within prior to calling the optimizer in the objects Lb and Ub, which stand for lower-bound and upper-bound, respectively: $Lb = [0, 0]$, $Ub = [1, 2\pi]$.

The process for the implementation of PSO is as follows:

a). Set the current iteration generation $G_c = 1$. Initialize a population which includes m particles. The ith particle has a random position in a specified space. For the dth dimension of V_i, $v_{id} = rand_2() \times v_{\max,d}$, where $rand_2()$ is a random value in the range $[-1, 1]$;

b). Evaluate the fitness of each particle;

c). Compare the evaluated fitness value of each particle with its *pbest*. If the current value is better than *pbest*, then set the current location as the *pbest* location. Furthermore, if the current value is better than *gbest*, then reset *gbest* to the current index in the particle array;

d). Change the velocity and location of the particle according to the Equations (21) and (22), respectively;

e). $G_c = G_c + 1$, loop to step b) until a stop criterion is met. Usually a sufficiently good fitness value or G_c achieves a predefined maximum generation $G_{\max}$.

Figure 4 shows a flowchart diagram of the main steps of the particle swarm optimization algorithm.

The particle swarm optimization (PSO) includes the following parameters: number of particles m, inertia weight w, acceleration constants C_1 and C_2, maximum velocity $V_{\max}$. During the evolution process, the swarm might undergo an undesired diversity loss. Some particles became inactive. Therefore, they lost both the global and the local search capabilities in the next generations. A loss of such a type translates that the particle will only be flying within a small space. This occurs when the particle's location and *pbest* are close to *gbest* (if the *gbest* has not significant changes) and when its velocity is close to zero for all dimensions. In sum, the loss means that the possible flying cannot lead to a perceptible effect on its fitness. On the ground of the theory of self-organization postulated by Nicolis [26] advances that if the system is going to be in equilibrium, the evolution process will stagnate.

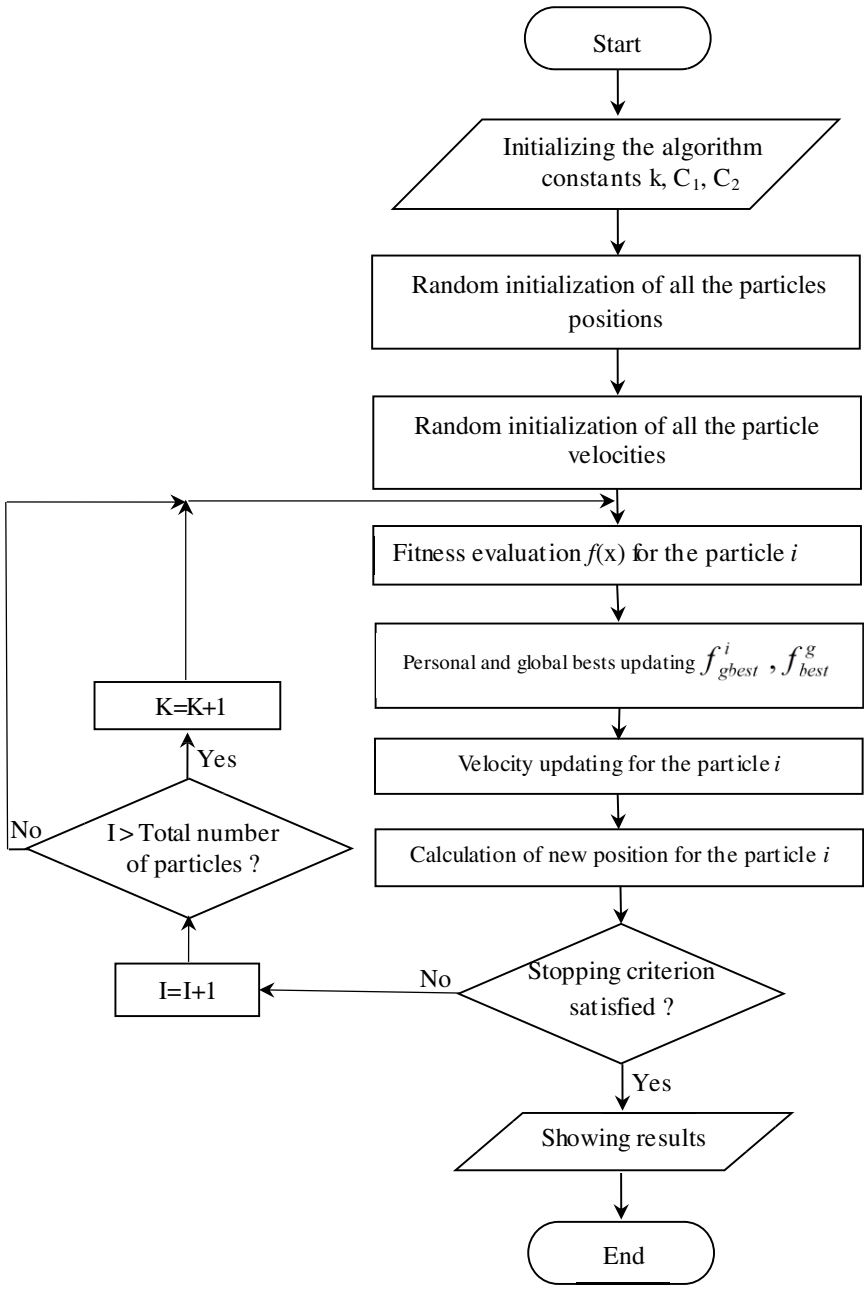

Figure 4. Flow-chart of the PSO algorithm.

If *gbest* is located at a local optimum, then the swarm will become premature convergence as all the particles become inactive. To stimulate the swarm with sustainable development, the inactive particle should adaptively be substituted by a fresh particle so as to keep the non-linear relations of feedback in Equation (21) efficient by maintaining the social diversity of the swarm. However, it is hard to identify the inactive particles, since the local search capability of a particle is highly depending on the specific location in the complex fitness landscape for different problems. Fortunately, the required precision of the fitness value is easily found from the fitness function The adaptive PSO is executed to replace the inactive particles by substituting step d) of the standard PSO process, by the pseudo code of the adaptive PSO that is shown in Figure 5.

```
int[ ]similar Count = new int[m];// at initialization stage
// Next code is employed to replace step d)
// in  standard PSO  process
For  (i = 0;i < m;i++)  {                    // for each particle
    IF (i ≠ g && |ΔF_i| < ε)
      THEN similar Count[i]++;               // add1
    ELSE similar Count[i] = 0;               // reset
    IF  (similar Count[i] > T_c)             // predefined count
      THEN replace (the i^th particle);
    ELSE execute (step d) in standard PSO
  }
```

Figure 5. Inserted pseudo code of adaptive PSO.

F_i is the fitness of the ith particle, F_{gbest} is the fitness of *gbest*, $\Delta F_i = f(F_i, F_{gbest})$, $f(x)$ is an error function, ε a predefined critical constant, depending on the required precision. T_c is the count constant. The replace () function is used to replace the ith particle, where X_i and V_i are reinitialized using the process in step a) of standard PSO, and its *pbest* is equal to X_i. The array *similar Count[i]* is employed to store the counts which successively satisfy the condition $|\Delta F_i| < \varepsilon$ for the ith particle which is not *gbest*. The inactive particle naturally satisfies the replace condition; however, if the particle is not inactive, it has less chance to be replaced as T_c increases. For adaptive particle swarm optimizer (APSO), ΔF_i is set as a relative error function, which is $(F_i - F_{gbest})/Min(abs(F_i), abs(F_{gbest}))$, where $abs(x)$ is the absolute value of x, $Min(x_1, x_2)$ the minimum value between x_1 and x_2. The critical constant ε is set to 0.0001, and the count constant T_c to 3. For the problem at hand, the number of dimensions is equal to twice the number of antenna elements, because both the amplitude and the phase of each parameter must be specified by the PSO. A swarm of 40 particles was used. The algorithm parameters C_1 and C_2 specify the relative weight that the global best position has versus the particle's own best. Empirical testing has found that 0.5 is a reasonable value for both C_1 and C_2. Linear velocity damping was applied with the upper limit equal to 0.9. Velocity damping improves the convergence behavior of the particle swarm by gradually increasing the relative emphasis of the global and own best positions on a particle's velocity. The upper limit of the inertia weight is 0.9 and the lower limit is 0.4.

4. NUMERICAL RESULTS

The synthesis technique, presented in this section, aims at optimizing a multibeam linear uniform array so that its main lobes occur exactly at certain specific angles, with maximum tolerance on the sidelobe levels using, complex weight excitations. The method has been used to design six uniform arrays for two modes TM_{11} and TM_{12}. Some numerical results of the optimized design of multibeam antenna arrays are reported in this paper. The simulation runs on an *HP* $i5$ laptop with a RAM of 4 GB. The algorithm of adaptive particle swarm optimization is implemented using Matlab code.

The antenna characteristics are as follows: $\varepsilon_r = 2.32$; $H_s = 1.59$ mm; r_1=35 mm; $r_2 = 70$ mm The case of an array with 12 elements and 0.5λ spacing is introduced. This array is supposed to generate two beams directed at the two angles 20° and −20°, for the two modes TM_{11} and TM_{12}, respectively. The requirements of the sector beam pattern with sidelobe levels are below than −20 dB, with two main beams directed toward the angles 20° and −20° as portrayed in Figures 6(a) and 6(b). Both figures show the normalized output pattern in dB, and the relative amplitudes of the two beams which are equal to unity for both modes. The maximum side-lobes levels are equal to −17.09 dB and −18.06 dB for the TM_{11} and TM_{12} modes respectively. For the design results of amplitude-phase synthesis, the adaptive particle swarm optimizer is run for 79 iterations and 155 iterations for the modes TM_{11} and TM_{12}; the CPU time is 10.64 and 20.87 minutes respectively, as demonstrated in Figures 7(a) and 7(b). The distribution of the amplitude and phase excitation law of the radiating elements in the periodic array is shown in Table 1.

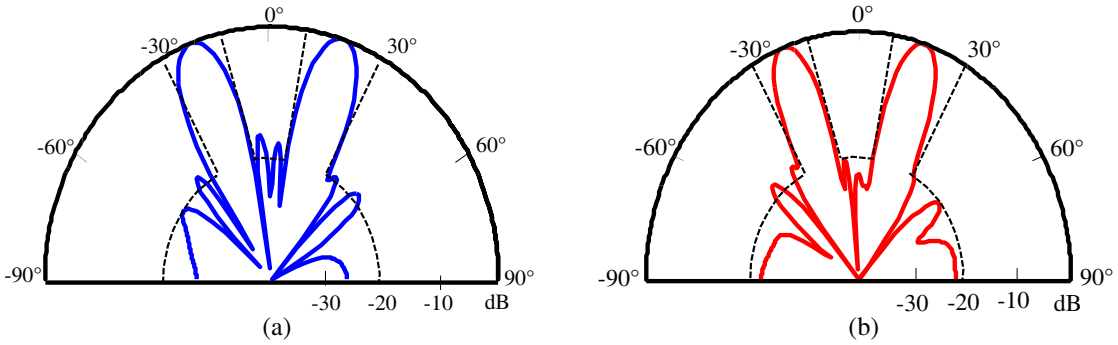

Figure 6. Simulation synthesis results. (a) Normalized pattern for TM_{11} Mode excitation. (b) Normalized pattern for TM_{12} mode excitation. The dashed lines are the desired sector beam patterns which have prescribed sidelobe levels below than -20 dB and with two main beams directed toward the angles $20°$ and $-20°$.

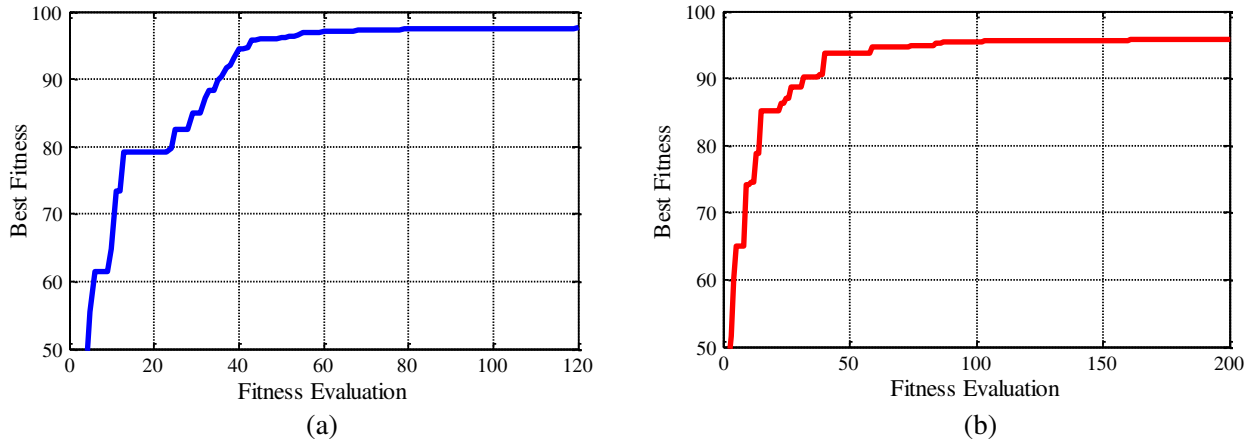

Figure 7. (a) The convergence curve TM_{11}. (b) The convergence curve TM_{12}.

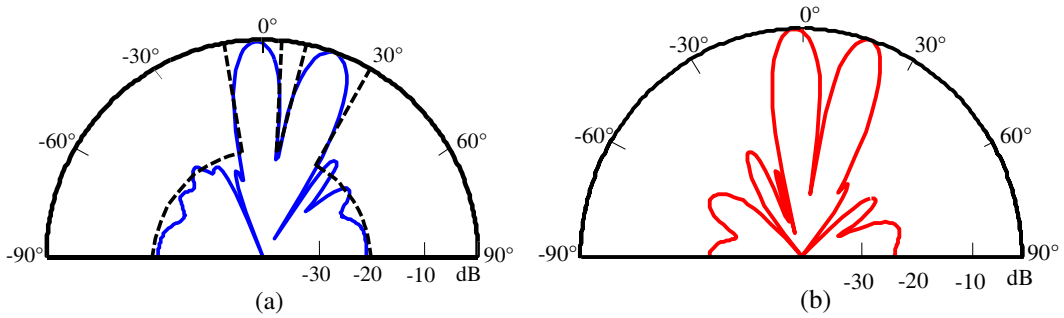

Figure 8. Simulation synthesis results. (a) Normalized pattern for TM_{11} Mode excitation. (b) Normalized pattern for TM_{12} mode excitation. The dashed lines are the desired sector beam patterns which have prescribed sidelobe levels below than -20 dB with two main beams directed toward the angles $0°$ and $20°$.

The second example belongs to the synthesis of a 12 radiators linear array, where the amplitudes and phases are modified. The adaptive particle swarm optimization is able to produce patterns with two prescribed main lobes, at around $0°$ and $20°$ for both modes TM_{11} and TM_{12}, while limiting the side-lobes level. The requirements of the sector beam pattern are shown in Figure 8. The amplitude-

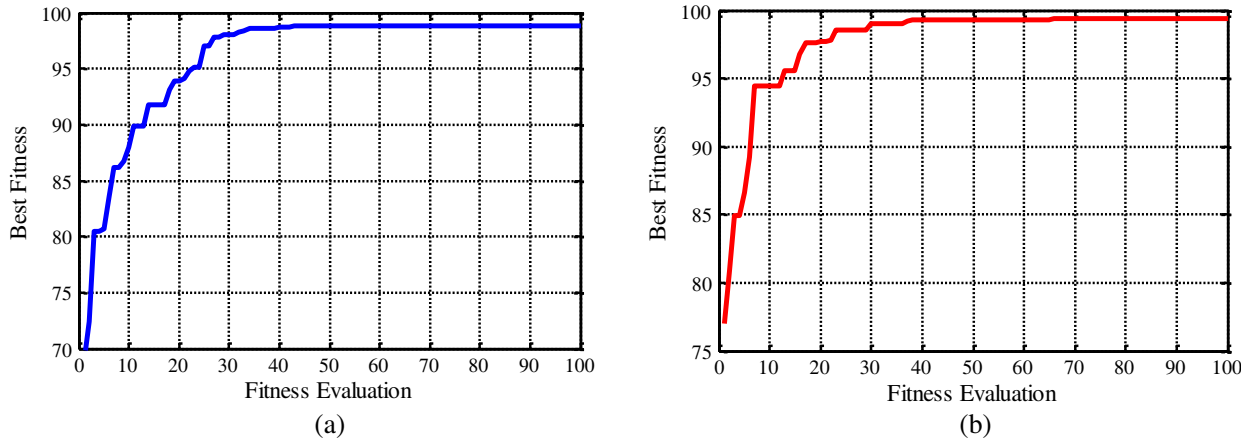

Figure 9. (a) The convergence curve TM_{11}. (b) The convergence curve TM_{12}.

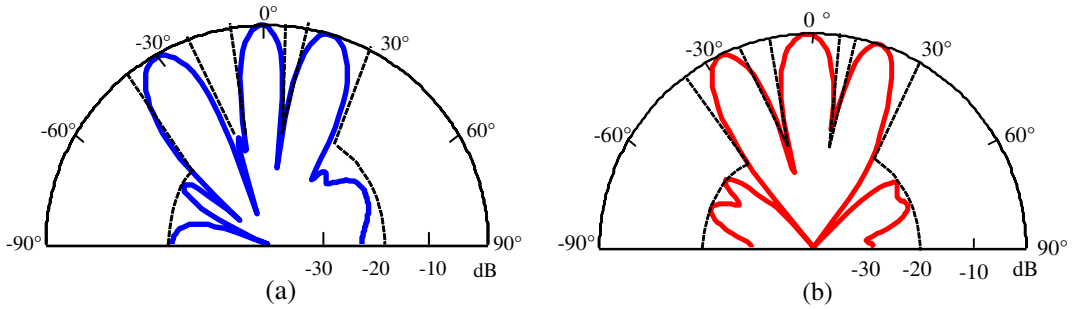

Figure 10. Simulation synthesis results. (a) Normalized pattern for TM_{11} Mode excitation. (b) Normalized pattern for TM_{12} mode excitation. The dashed lines are the desired sector beam pattern which have prescribed sidelobe levels below than -20 dB with three main beams directed toward the angles $-30°$, $0°$ and $20°$.

phase synthesis gave the maximum side-lobe levels of 18 dB and -19.50 dB, for the two modes TM_{11} and TM_{12} respectively. The adaptive particle swarm optimization was run for 100 iterations for the two modes as shown in Figure 9, with an initial population of 40 particles; the required execution time is 5.79 and 8.89 minutes for the TM_{11} and TM_{12} respectively. The optimized excitation magnitudes and phases of the array elements are shown in Table 1.

The third numerical example refers to the same array and is obtained by imposing three maxima along the desired directions. It can be noticed that, when the proposed algorithm is used, the beams can be oriented exactly in the required directions. The applied method yielded the patterns shown in Figures 1(a) and (b), for TM_{11} and TM_{12} modes, respectively. The requirements of such sector beam pattern are graphically presented in Figure 10. After 100 and 220 iterations, the fitness value reached its maximum and the optimization process ended due to meeting the design goal for both modes TM_{11} and TM_{12} the exact execution time is 14.01 and 30.82 minute respectively. The fitness convergence curves are presented in Figures 11(a) and (b). The synthesis results obtained for the two modes TM_{11} and TM_{12} are depicted in Table 1.

Table 1 shows the optimized element excitations for all linear antenna array designs discussed above.

Our proposed method can be extended to the planar antenna array which consists of 10×10 annular ring antennas equally spaced by 0.5λ along the directions Ox and Oy. The synthesis objective was to obtain a pattern with two narrow beams in the desired directions for the modes TM_{11} and TM_{12} in the principal plane (E-plane $\varphi = 0°$) by acting on the amplitudes and phases of sources while achieving a minimum peak sidelobe levels. Satisfactory results were obtained and multibeam patterns were achieved and plotted in the polar coordinate system, as shown in Figures 12(a) and (b). The

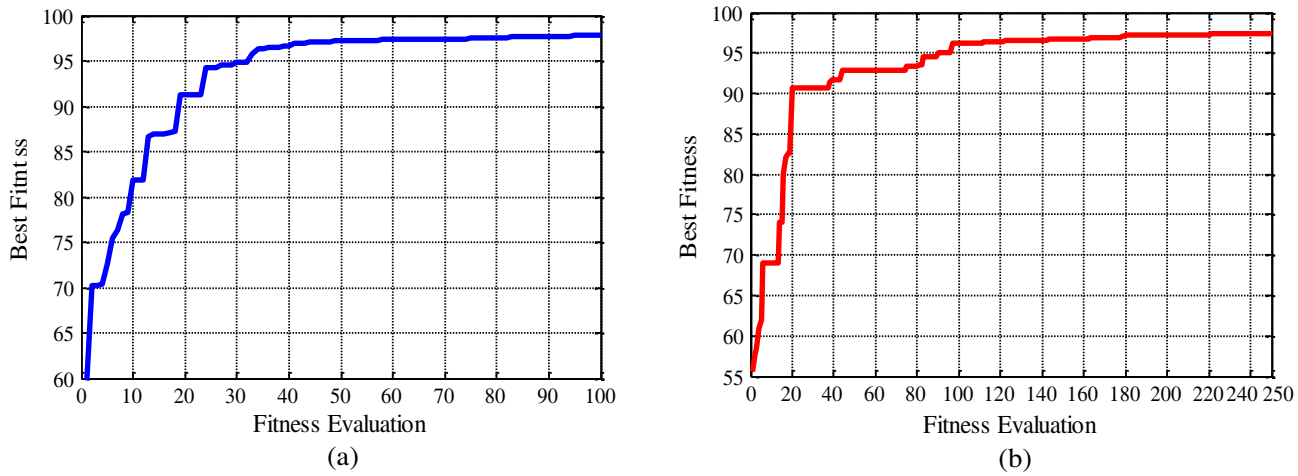

Figure 11. (a) The convergence curve TM_{11}. (b) The convergence curve TM_{12}.

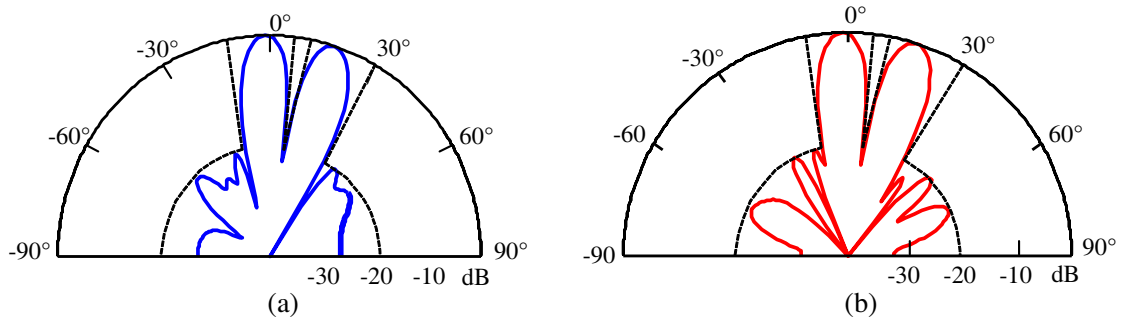

Figure 12. (a) Normalized pattern TM_{11}. (b) Normalized pattern TM_{12}. The dashed lines are the desired sector beam pattern which have prescribed sidelobe levels below than -20 dB with two main beams directed toward the angles 0° and 20°.

Table 1. Optimized excitations obtained with APSO for linear arrays.

	Figure 6				**Figure 8**				**Figure 10**			
N°	**TM_{11}**		**TM_{12}**		**TM_{11}**		**TM_{12}**		**TM_{11}**		**TM_{12}**	
	Ampl (Volt)	**Phase (Rad)**	**Ampl (Volt)**	**Phase (Rad)**	**Ampl (Volt)**	**Phase (Rad)**	**Ampl (Volt)**	**Phase (Rad)**	**Ampl (Volt)**	**Phase (Rad)**	**Ampl (Volt)**	**Phase (Rad)**
1	0.2814	1.5321	0.4795	3.7084	0.1172	2.2310	0.2201	2.7581	0.0073	2.4007	0.1547	2.0456
2	0.5192	1.4963	0.5666	3.6196	0.2183	1.8209	0.2761	1.4984	0.0706	2.4494	0.3306	4.8580
3	0.0628	5.1279	0.9796	0.5862	0.1025	4.9695	0.2839	5.2853	0.3766	3.2325	0.3693	6.1627
4	0.7214	4.7912	0.9075	0.9202	0.5698	3.6570	0.5143	4.6853	0.8339	3.8514	0.5590	1.8092
5	0.6692	4.8370	0.3934	3.5280	0.9016	3.1761	0.7953	4.1869	0.3684	3.4844	0.8317	3.0304
6	0.0722	2.3679	0.8283	4.4429	0.9974	2.5947	0.6662	3.4443	0.6434	2.1487	0.2994	3.7045
7	0.7842	1.7826	0.4545	4.1771	0.6872	2.2393	0.6900	3.0203	0.7342	2.5638	0.5487	0.4598
8	0.5393	1.9761	0.1492	3.1116	0.2607	1.4994	0.1721	5.4527	0.5271	4.8216	0.5377	1.2848
9	0.1288	4.7838	0.6615	0.7736	0.6661	4.3732	0.5743	6.0291	0.7721	5.2835	0.5047	3.5016
10	0.4977	5.1351	0.6034	1.5027	0.8003	4.0110	0.7458	4.8610	0.3017	3.8874	0.7383	3.7786
11	0.3584	5.3536	0.2782	3.7525	0.8521	3.4245	0.8896	4.3904	0.8238	3.4586	0.2953	2.6360
12	0.0829	2.4152	0.3365	4.7316	0.6125	2.9748	0.3209	3.5256	0.3704	3.7639	0.3482	1.7061

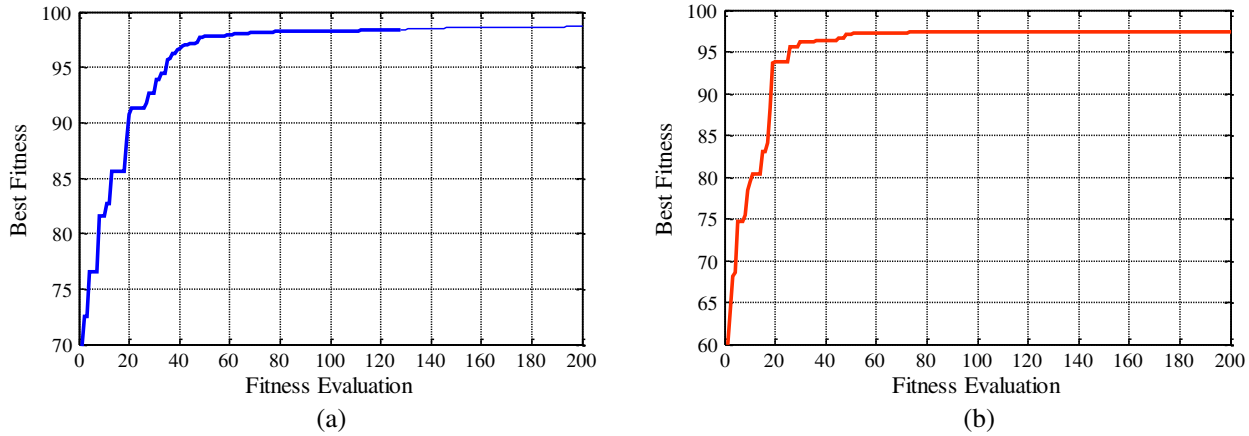

Figure 13. (a) The convergence curve TM_{11}. (b) The convergence curve TM_{12}.

Table 2. Optimized excitations obtained with APSO for planar array.

N°	Figure 12 (a)				Figure 12 (b)			
	TM_{11}				TM_{12}			
	Amp.*Ox* (Volt)	Amp.*Oy* (Volt)	Phase.*Ox* (Rad)	Phase.*Oy* (Rad)	Amp.*Ox* (Volt)	Amp.*Oy* (Volt)	Phase.*Ox* (Rad)	Phase.*Oy* (Rad)
1	0.3604	0.7314	4.0940	3.1520	0.6070	0.2450	2.4543	1.5120
2	0.6551	0.6374	3.6752	4.0978	0.9297	0.2423	1.7174	4.2740
3	0.7987	0.3496	2.9905	3.0617	0.5070	0.6524	0.7058	2.3789
4	0.5570	0.7053	2.8384	2.1905	0.2072	0.3348	0.6830	2.2938
5	0.1523	0.6106	2.3925	1.5310	0.1606	0.6216	3.3935	3.5386
6	0.3387	0.4968	5.1595	3.9306	0.5374	0.4853	3.4524	1.9370
7	0.7194	0.3309	4.3831	1.6232	0.9036	0.6509	2.7330	3.4076
8	0.7426	0.5672	3.9702	2.9599	0.6907	0.4821	1.6403	2.8137
9	0.5846	0.2113	3.5105	2.5016	0.3776	0.9998	0.7967	2.4105
10	0.2120	0.4651	3.2002	4.3735	0.2634	0.3771	3.9290	3.6162

Table 3. CPU execution time and iteration value at convergence of the APSO algorithm.

	Figure 6		Figure 8		Figure 10		Figure 12	
	TM_{11}	TM_{12}	TM_{11}	TM_{12}	TM_{11}	TM_{12}	TM_{11}	TM_{12}
CPU Execution times (min.)	10.64	20.87	5.79	8.89	14.01	30.82	27.31	28.60
Iteration value at Convergence	79	155	43	66	100	220	191	200

excitation amplitudes and phases of the elements for TM_{11} and TM_{12} are shown in Table 2. For the design specifications, the modified particle swarm optimization method is run for 191 and 200 iterations, for TM_{11} and TM_{12} modes as reported in Figures 13(a) and (b), respectively. The execution time is equal to 27.31 minutes for TM_{11} and 28.60 minutes for TM_{12}.

The synthesis examples show the principal characteristics of the suggested method. These arrays meet strict demands, especially in terms of maximum directivity to be guaranteed in the selected angles and the sidelobe levels to be kept below an a desired value. The adaptive particle swarm optimization synthesis results of magnitudes and phases of the case of planar dual-beam array are given in Table 2.

The measured CPU execution time required to reach convergence by the APSO algorithm is shown in Table 3.

5. CONCLUSION

In this paper, the adaptive particle swarm optimization algorithm is introduced with the end to synthesize the multibeam linear and planar annular ring antenna arrays for the TM_{11} and TM_{12} modes. The complex weights of the arrays were calculated so as to approach the appropriate radiance diagram. Satisfactory side-lobe levels were obtained while high directivities and narrow beams were attained. Results indicate a very good agreement between the expected and synthesized specifications, for the two modes. Significant results show the effectiveness of the suggested adaptive swarm optimization algorithm through the determination of the optimized complex weight vectors.

REFERENCES

1. Morabito, A. F., T. Isernia, and L. Di Donato, "Optimal synthesis of phase-only reconfigurable linear sparse arrays having uniform-amplitude excitations," *Progress In Electromagnetics Research*, Vol. 124, 405–423, 2012.
2. Didouh, S., M. Abri, and H. Abri Badaoui, "A new C and Ku-band logarithmically periodic linear bowtie antennas array design using lumped-element equivalent schematic model," *International Journal of Electronics and Communications*, Vol. 69, 1766–1772, 2015.
3. Gopi, R., M. Durbadal, K. Rajib, and S. Ghoshal, "Directivity maximization and optimal far-field pattern of time modulated linear antenna arrays using evolutionary algorithms," *International Journal of Electronics and Communications*, Vol. 69, 1800–1809, 2015.
4. Lakshman, P. and D. Ghosh, "Linear antenna array synthesis using cat swarm optimization," *International Journal of Electronics and Communications*, Vol. 68, 540–549, 2014.
5. Abri, M., N. Boukli-hacene, F. T. Bendimerad, and E. Cambiaggio, "Design of ring printed antennas array for dual band," *Microwave Journal*, Vol. 49, 228–232, 2006.
6. Jana, R. and R. Bhattacharjee, "Matched feed design employing TE_{01} and TM_{11} modes in a smoothwalled rectangular waveguide for cross-polar reduction in offset reflector antenna systems," *International Journal of Electronics and Communications*, Vol. 69, 873–877, 2015.
7. Dahele, J. S. and K. F. Lee, "Theory and experiment on microstrip antennas with airgaps," *Proceeding of IEE*, 455–460, 1985.
8. Deschamps, G. A., "Microstrip microwave antennas," *Proc. 3rd USAF Symposium on Antennas*, 1953.
9. Urvinder, S. and S. Rohit, "Optimal synthesis of linear antenna arrays using modified spider monkey optimization," *Arabian Journal for Science and Engineering*, Vol. 41, No. 8, 2957–2973, 2016.
10. Bilel, H., L. Selma, and A. Taoufik, "Uniform and concentric circular antenna arrays synthesis for smart antenna systems using artificial neural network algorithm," *Progress In Electromagnetics Research B*, Vol. 67, 91–105, 2016.
11. Prerna, S. and K. Ashwin, "Optimal pattern synthesis of linear antenna array using grey wolf optimization algorithm," *International Journal of Antennas and Propagation*, Vol. 2016, Article ID 1205970, 11, 2016.
12. Chaker, H., S. M. Meriah, and F. T. Bendimerad, "Synthesis of multibeam antennas arrays with a modified particle swarm optimization algorithm," *The International Arab Journal of Information Technology*, Vol. 7, 250–255, 2010.
13. Chaker, H., "Null steering and multi-beams design by complex weight of antennas array with the use of APSO-GA," *WSEAS Transactions on Communications*, Vol. 13, 99–108, 2014.
14. Robinson, J. and Y. Rahmat-Samii, "Particle swarm optimization (PSO) in electromagnetics," *IEEE Transactions on Antennas and Propagation*, Vol. 52, 397–407, 2004.

15. Khodier, M. M. and C. G. Christodoulou, "Linear array geometry synthesis with minimum sidelobe level and null control using particle swarm optimization," *IEEE Transactions on Antennas and Propagation*, Vol. 53, 2674–2679, 2005.
16. Pappula, L. and D. Ghosh, "Linear antenna array synthesis for wireless communications using particle swarm optimization," *15th International Conference on Advanced Computing Technologies*, 780–783, 2013.
17. Schlosser, E. R., S. M. Tolfo, and M. V. T. Heckler, "Particle swarm optimization for antenna arrays synthesis," *IEEE Microwave and Optoelectronics Conference*, 1–6, Nov. 2015.
18. Abri, M., N. Boukli-hacene, and F. T. Bendimerad, "Ring printed antennas arrays radiation. Application to multibeam," *Mediterranean Microwave Symposium-mms*, 2004.
19. Abri, M., N. Boukli-hacene, and F. T. Bendimerad, "Application du recuit simulé à la synthèse d'antennes en réseau constituées d'éléments annulaires imprimés," *Annales des Télécommunications*, Vol. 60, 1424–1440, 2005.
20. Abri, M., N. Boukli-hacene, and F. T. Bendimerad, "Application of the genetic algorithm to the ring printed antennas arrays synthesis," *International Journal of Modelling and Simulation*, Vol. 28, 174–181, 2008.
21. Mailloux, R. J., *Electronically Scanned Array*, Morgan and Claypool Pub., 2007.
22. Xie, X.-F., W.-J. Zhang, and Z.-L. Yang, "Adaptive particle swarm optimization on individual level," *International Conference on Signal Processing*, 1215–1218, 2002.
23. Eberhart, R. and Y. Shi, "Particle swarm optimization: developments, applications and resources," *IEEE International Conference Evolutionary Computation*, Vol. 1, 81–86, 2001.
24. Kennedy, J., "The particle swarm: social adaptation of knowledge," *IEEE International Conference Evolutionary Computation*, 303–308, 1997.
25. Kennedy, J. and R. Eberhart, "Particle swarm optimization," *IEEE Conference on Neural Networks*, Vol. 4, 1942–1948, 1995.
26. Nicolis, G. and I. Prigogine, *Self-organization in No Equilibrium Systems: From Dissipative Systems to Order Through Fluctuations*, John Wiley, 1977.